NACA TN No. 1824

NATIONAL ADVISORY COMMITTEE FOR AERONAUTICS

TECHNICAL NOTE

No. 1824

LINEARIZED COMPRESSIBLE-FLOW THEORY FOR SONIC FLIGHT SPEEDS

By Max. A. Heaslet, Harvard Lomax, and
John R. Spreiter

Ames Aeronautical Laboratory,
Moffett Field, Calif.

Washington
March 1949

TABLE OF CONTENTS

NATIONAL ADVISORY COMMITTEE FOR AERONAUTICS

TECHNICAL NOTE NO. 1824

LINEARIZED COMPRESSIBLE-FLOW THEORY FOR SONIC FLIGHT SPEEDS

By Max. A. Heaslet, Harvard Lomax, and
John R. Spreiter

SUMMARY

The partial differential equation for the perturbation velocity potential is examined for free-stream Mach numbers close to and equal to one. It is found that, under the assumptions of linearized theory, solutions can be found consistent with the theory for lifting-surface problems both in stationary three-dimensional flow and in unsteady two-dimensional flow. Several examples are solved including a three-dimensional swept-back wing and a two-dimensional harmonically oscillating wing, both for a free-stream Mach number equal to one.

INTRODUCTION

Much of the recent progress in the theoretical analysis of compressible-flow fields is attributable to the successful application of linearization methods. Although the basic assumptions used in conventional linearized theory appear at first glance to be highly restrictive, it has been found that, just as in the analogous case of thin-airfoil theory for incompressible flow, the methods have many fields of utilization adequate for most engineering purposes. Since the basic methods are so well known and depend on such relatively simple mathematical tools, it appears obvious that the range of applicability of the theory should be explored completely. Such is the purpose of the present report. It has been more or less tacitly presumed in the past that such applications cannot treat cases for which the flight velocity is near the speed of sound. In the study of two-dimensional steady-state problems in airfoil theory, this presumption is certainly true. The Prandtl-Glauert and Ackeret rules for variation of pressure coefficient with free-stream Mach number in the subsonic and supersonic regimes, respectively, are clearly invalid for Mach numbers near one, since perturbation velocities

become arbitrarily large. In this case, linearized theory therefore predicts its inability to treat such problems. On the other hand, if linear methods are applied to nonstationary two-dimensional airfoil and particular steady-state, three-dimensional, lifting-surface problems at sonic speeds, a consistent theory results since solutions are found which yield perturbation velocities of the same order of magnitude as those calculated for free-stream Mach numbers of, say, 0.6 or 1.5.

Unfortunately, arbitrary thickness distributions at sonic speeds cannot be studied by linear theory in the steady state since, in general, the theory predicts infinite pressure differences between the wing surface and infinity. In the particular case of a yawed, symmetrical wing of infinite aspect ratio, the results are, however, again consistent with the theory and yield pressure distributions which are the same as those determined by using only the component of free-stream velocity normal to the leading edge. The derivation of this latter result for a free-stream Mach number of one will be given.

The difficulty of not being able to include thickness effects in general, together with the uncertainty of the magnitude of the viscous effects, leaves the question as to the limitations of such a linear theory in application to practical wing shapes. Such a question can certainly not be resolved by mathematical reasoning alone. The extent to which the fluid medium can be idealized at these speeds is left, for the time being, unsettled and it remains for experiment to determine whether the consistent mathematical results which are obtained from the linearized equations provide reasonably exact predictions. In this connection, it should be mentioned that the few experimental results available for the total lift on thin triangular wings at Mach numbers near one tend to confirm the theory. But even if more detailed experimental results indicate that further refinements are necessary, there is still little doubt but that the linear potential solutions will provide a valuable basis for more exact extensions of theory.

The present report is divided into three parts. In the first part, the linearizatien of the partial differential equation for the velocity potential is carried out in some detail for steady-state conditions. A by-product of this derivation is the nonlinear form of the equation for two-dimensional flow which was used by von Kármán (reference 1) to determine his similarity rules for transonic flow. The equation for unsteady two-dimensional flow based on the same assumptions is also given. The second part of the report

is restricted to two-dimensional unsteady problems for values of Mach number near one. The principal contribution of this section is the evaluation of the change with time of the pressure distribution over an airfoil starting suddenly from rest at a speed close to that of sound. Such an idealized problem involves a step function in velocity in which the airfoil has zero velocity for all negative values and near sonic velocity for all positive values of time. From these results the initial build-up of lift can be calculated for Mach numbers near one, although the eventual value of the lift cannot be found by linear methods. Further application can also be made to problems in flutter and gust loads. The third part of the report treats the steady-state three-dimensional problem. Both lifting surfaces and symmetrical nonlifting wings are considered and it is seen that in the former case consistent solutions are obtained by particularly simple means. These solutions represent the limiting case of both subsonic and supersonic lifting-surface theory and give, for example, the same value of lift-curve slope at the speed of sound that was obtained for the supersonic triangular wing by Stewart (reference 2).

A list of symbols is given in the appendix.

PART I - THE LINEARIZED EQUATIONS OF MOTION

Steady State

The nonlinear partial differential equation satisfied by the velocity potential Φ of an isentropic flow field can be expressed in the form

$$\Phi_{xx}\left(1-\frac{\Phi_x^2}{a^2}\right)+\Phi_{yy}\left(1-\frac{\Phi_y^2}{a^2}\right)+\Phi_{zz}\left(1-\frac{\Phi_z^2}{a^2}\right)$$
$$-\frac{2}{a^2}\Phi_{yz}\Phi_y\Phi_z-\frac{2}{a^2}\Phi_{zx}\Phi_z\Phi_x-\frac{2}{a^2}\Phi_{xy}\Phi_x\Phi_y=0 \qquad (1)$$

where the subscript notation is used to indicate differentiation and a is the local speed of sound given by the relation

$$\left(\frac{a}{V_o}\right)^2=\frac{1}{M_o^2}\left\{1-\frac{(\gamma-1)}{2}M_o^2\left[\left(\frac{V}{V_o}\right)^2-1\right]\right\} \qquad (2)$$

In this latter equation V_o and M_o are, respectively, velocity and Mach number of the free stream, γ is the ratio of specific

heats (for air, γ=1.4), and V is local velocity.

Introducing the perturbation velocity potential φ, where

$$\varphi = -V_o x + \Phi \tag{3}$$

it is possible to express equation (1) in terms of the derivatives of φ and the parameters M_o and V_o. To begin the linearization of the resulting equation, the coefficients of the second ordered derivatives of Φ are expanded in Maclaurin series with ascending powers of $\frac{u}{V_o}$, $\frac{v}{V_o}$, $\frac{w}{V_o}$. The convergence is assured provided

$$\left| \frac{(\gamma-1)}{2} M_o^2 \left(\frac{2u}{V_o} + \frac{u^2+v^2+w^2}{V_o^2} \right) \right| < 1 \tag{4}$$

or, in a slightly modified form, provided

$$\left| V^2 - V_o^2 \right| < \frac{2a_o^2}{\gamma-1} = 5a_o^2 \tag{5}$$

If the assumption is now made that $\frac{u}{V_o}$, $\frac{v}{V_o}$, $\frac{w}{V_o} \ll 1$ so that second and higher powers in the perturbation velocities can be neglected in comparison with one, the partial differential equation can be simplified to the form

$$\varphi_{xx} \left\{ 1 - M_o^2 \left[1 + \frac{2u}{V_o} + (\gamma-1) M_o^2 \frac{u}{V_o} \right] \right\} + \varphi_{yy} + \varphi_{zz}$$

$$- 2 \varphi_{xz} \frac{w}{V_o} M_o^2 - 2 \varphi_{xy} \frac{v}{V_o} M_o^2 = 0 \tag{6}$$

From this equation all the succeeding expressions will be derived.

Two- and three-dimensional linear equations, $M_o \neq 1$. - Since equation (6) is obviously nonlinear, additional assumptions must be made to reduce it to a linear form. Clearly, these assumptions must involve the relative magnitudes of all the terms in order to determine which ones may be neglected. Perhaps one of the least restrictive set of conditions is that:

(a) The ratios of the perturbation velocities to the free-stream velocity are small enough to be neglected when compared to one.

(b) The velocity gradients at a given point of the flow field are all of similar magnitude.

With the aid of these assumptions, it follows that, to the order of the approximations made, the perturbation velocity potential φ satifies the well-known linear equation

$$(1 - M_o^2)\,\varphi_{xx} + \varphi_{yy} + \varphi_{zz} = 0 \tag{7}$$

In the case of two-dimensional flow, the equation is independent of y and thus may be written in the form

$$(1 - M_o^2)\,\varphi_{xx} + \varphi_{zz} = 0 \tag{8}$$

Two- and three-dimensional nonlinear equations, $M_o = 1$. - The study of equation (8) in both subsonic and supersonic flow has shown that for arbitrary lifting surfaces or symmetrical nonlifting airfoils the value of the induced velocity u on the surface of a fixed geometric configuration is proportional to $(|1 - M_o^2|)^{-1/2}$. In all airfoil problems, the value of u becomes infinitely large as M_o approaches one, either from above or below, and the basic assumptions are thus violated. Such a difficulty led Oswatitsch and Wieghardt (reference 3) and Sauer (reference 4) to abandon the restriction of linearity and to seek a more exact equation at $M_o = 1$. Retaining the assumptions underlying equation (6) and setting $V_o = a^*$ where a^* is the critical speed of sound, it follows that at $M_o = 1$ the perturbation velocity potential satisfies the equation

$$\frac{(\gamma+1)}{a^*}\,\varphi_x\,\varphi_{xx} - \varphi_{zz} + \frac{2}{a^*}\,\varphi_z\,\varphi_{xz} = 0 \tag{9}$$

Since φ_x is much larger than φ_z as the Mach number approaches one, equation (9) may be further simplified to

$$\frac{(\gamma+1)}{a^*}\,\varphi_x\,\varphi_{xx} - \varphi_{zz} = 0 \tag{10}$$

If, in three dimensions, the perturbation velocities do not remain small, equation (6) again supplies the necessary form of the differential equation at $M_o = 1$. From the relation $V_o = a^*$, the

required expression is

$$\frac{(\gamma+1)}{a^*}\varphi_x\varphi_{xx} - \varphi_{yy} - \varphi_{zz} + \frac{2}{a^*}\varphi_z\varphi_{xz} + \frac{2}{a^*}\varphi_y\varphi_{xy} = 0 \qquad (11)$$

Two- and three-dimensional linear equations, $M_o = 1$. —

Equation (10) has been used by von Kármán (reference 1) to establish similarity rules for two-dimensional transonic flow and is the basis for work continuing at the present time. (See also reference 5.) If at $M_o = 1$ the assumptions made in the linearization process still hold, it follows from either equation (10) or (8) that the differential equation reduces to the form

$$\varphi_{zz} = 0 \qquad (12)$$

It is possible, however, to predict independently from this relation that linearized methods cannot be applied to the calculation of arbitrary airfoil pressure distributions. The range of applicability of such an equation is thus almost nonexistent. On the other hand, the linearized form of equation (11) or (7) at $M_o = 1$ is

$$\varphi_{yy} + \varphi_{zz} = 0 \qquad (13)$$

and from this equation a class of nontrivial solutions can be obtained for particular boundary conditions. Both equations are of parabolic form in the number of dimensions for which they are defined. In the present report, formal solutions satisfying the imposed conditions will be obtained in three dimensions for flat lifting surfaces with swept-back leading edges and for an infinitely long, symmetrical, swept-back wing.

Unsteady State

The derivation of the steady-state equations for the velocity potential was developed in some detail because of the various results to be obtained. Similar methods can be used when unsteady conditions are to be considered, the differential equation for the velocity potential being now in the form

$$-\frac{1}{a^2}\left(\Phi_{t't'} + 2\Phi_x\Phi_{xt'} + 2\Phi_y\Phi_{yt'} + 2\Phi_z\Phi_{zt'}\right) + \Phi_{xx}\left(1 - \frac{\Phi_x^2}{a^2}\right) + \Phi_{yy}\left(1 - \frac{\Phi_y^2}{a^2}\right) + \Phi_{zz}\left(1 - \frac{\Phi_z^2}{a^2}\right) - \frac{2}{a^2}\Phi_{yz}\Phi_y\Phi_z - \frac{2}{a^2}\Phi_{zx}\Phi_z\Phi_x - \frac{2}{a^2}\Phi_{xy}\Phi_x\Phi_y = 0 \qquad (14)$$

where t' represents time. The details of the derivation can, however, be avoided by referring directly to the equation satisfied by the velocity potential for the propagation of sound waves of small amplitude. (See reference 6, p. 492.) In this form of the equation the Cartesian coordinate system x, y, z is assumed fixed in the medium so that free-stream velocity is zero, while the wing, which moves in the direction of the negative x axis with velocity V_o, generates small pressure disturbances. As a consequence, the velocity potential of the field satisfies the well-known wave equation in three space dimensions:

$$\frac{1}{a^2}\varphi_{t't'} - \varphi_{xx} - \varphi_{yy} - \varphi_{zz} = 0 \tag{15}$$

Equation (15) is reducible to canonical form by means of the relation

$$t = a_o t'$$

and the three-dimensional form of the equation is therefore

$$\varphi_{tt} - \varphi_{xx} - \varphi_{yy} - \varphi_{zz} = 0 \tag{16}$$

while in the two-dimensional case independence with respect to y yields

$$\varphi_{tt} - \varphi_{xx} - \varphi_{zz} = 0 \tag{17}$$

PART II. TWO-DIMENSIONAL LINEAR PROBLEMS FOR M_o NEAR ONE

Unsteady State, $M_o \gtrless 1$

It was pointed out in the derivation of equation (12) that the linear equation for the velocity potential is not applicable to airfoil problems in either the subsonic or supersonic regimes for M_o near one. The possibility still remains, however, of analyzing unsteady flows during the period in which the perturbation velocities remain small. As an example of such a problem, consider the case of a flat lifting surface at a small angle of attack α starting from rest at a velocity V_o near the speed of sound. The perturbation potential for such a motion is equivalent to the change in potential brought about by an abrupt change α in angle of attack of an airfoil flying in a steady-state condition at velocity equal to V_o.

The change in load distribution brought about by this maneuver is the so-called indicial load distribution and a knowledge of such indicial functions is important for applications using operational calculus.

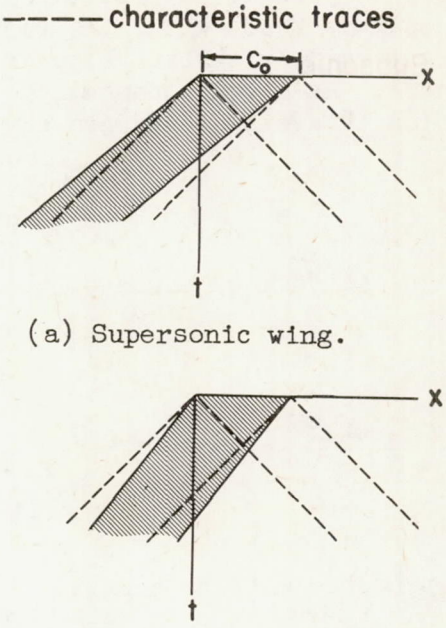

(a) Supersonic wing.

(b) Subsonic wing.

Figure 1.- Boundary conditions for two-dimensional unsteady-lift problem.

Figures 1(a) and 1(b) furnish an insight into the nature of the boundary conditions for airfoils traveling, respectively, at supersonic and subsonic speeds. The chord is initially on the x axis with leading edge at the origin and trailing edge at $x = c_o$. With increasing time, the wing section travels in the negative x direction and sweeps out a portion of the xt plane as shown in the figures (indicated by shaded areas). Throughout this part of the plane the boundary conditions require that the induced vertical velocity is $-V_o\alpha$, while elsewhere on the plane the induced velocities are continuous functions of z. In figure 2, sketches of the airfoil in the supersonic and subsonic cases are shown together with indications of the manner in which the disturbance field spreads. These wings are presented in xyz space with time as a parameter so that their coordinate system is not to be confused with that of figure 1. The airfoils are traveling from right to left at Mach numbers of 0.8 in the subsonic case and 1.2 in the supersonic case, and for a time corresponding to that required for the wing to travel a distance of one-third chord length. At $t = 0$ cylindrical waves are induced at each disturbance point, that is, at each point of the chord. These waves expand radially at the center of the expanding waves moves relative to the initial disturbance point. At a given instant in time the entire disturbance region

of the airfoil is contained within the closed surfaces shown in the figures, the outer surfaces corresponding to the largest values of

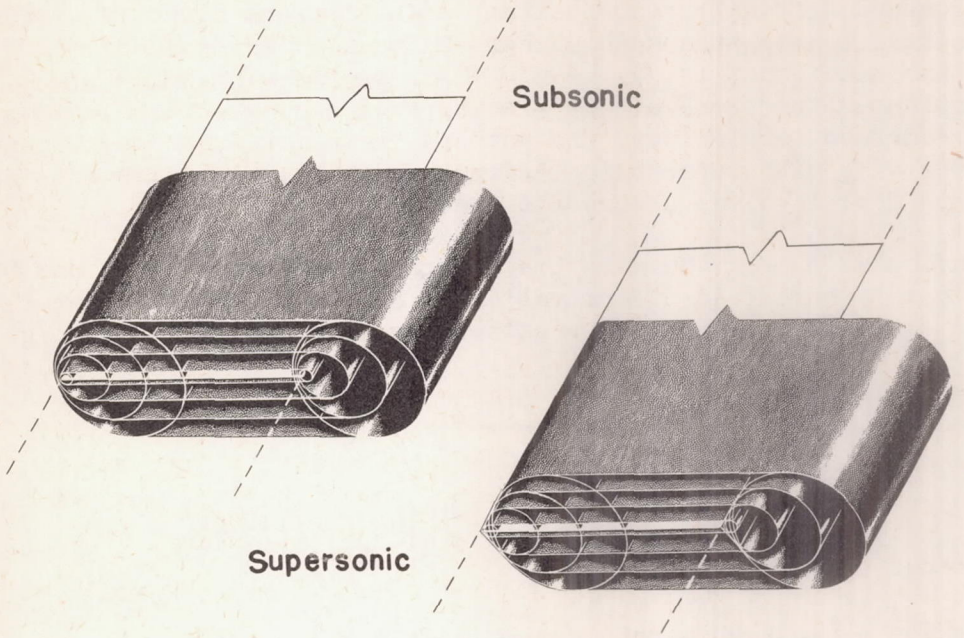

Figure 2.– Sketch showing extent of disturbance fields after travel of one–third chord length.

time. In the supersonic case, the pressure distribution over the wing reaches a steady–state value as soon as the wing moves ahead of the expanding cylindrical wave produced at $t = 0$ by the leading edge. In the subsonic case, the wing never leaves the disturbance field of the cylinders and, as will be seen later, the steady–state pressure distribution is approached asymptotically.

It is apparent from equation (17) that the characteristic cones have semivertex angles equal to 45° and that the cones with vertices on the xt plane have traces with slopes equal to ± 1. These cones determine the upstream boundary of the field of influence of the vertex point and their cross sections in the plane t = constant are the disturbance regions of the cylindrical waves arising at the vertex. Thus, perturbations in pressure produced initially at the leading edge of the wing section are confined at later time, in the modified coordinate system, to the cone with vertex at the origin and traces $x = \pm t$.

The solution of equation (17) for boundary values of the type under discussion has been indicated in reference 7 through consideration of an analogue problem in supersonic lifting-surface theory. Thus, the shaded areas in figures 1(a) and 1(b) are thought of as swept-forward lifting surfaces situated in a stream directed along the positive t axis at a Mach number $M_o = \sqrt{2}$. The boundary values remain the same; that is, $\varphi_z = w = -V_o\alpha$ on the wing and φ_t, φ_y, φ_z are continuous functions of z elsewhere in the xt plane. In lifting-surface terminology, the unsteady case for supersonic speed becomes a wing with supersonic leading edge, while the case indicated in figure 1(b) involves a subsonic leading edge.

The solution for the wing traveling at supersonic speed has been given in reference 7 in a form valid for all Mach numbers greater than or equal to one. The expressions for load coefficient $\Delta p/q$, where

$$\frac{\Delta p}{q} = \frac{p_l - p_u}{\frac{1}{2}\rho_o V_o^2}$$

differ analytically in various regions of the xt plane. These expressions are:

Region A (between lines $x = -M_o t$, $x = -t$)

$$\frac{\Delta p}{q} \quad \frac{4\alpha}{\sqrt{M_o^2 - 1}} \tag{18a}$$

Region B (between lines $x = -t$, $x = t$, and $x = c_o - M_o t$)

$$\frac{\Delta p}{q} = \frac{4\alpha}{\sqrt{M_o^2 - 1}}\left[\frac{1}{\pi} \arccos \frac{M_o x + t}{x + M_o t} + \frac{\sqrt{M_o^2 - 1}}{\pi M_o}\left(\frac{\pi}{2} + \arcsin \frac{x}{t}\right)\right] \tag{18b}$$

Region C (between lines $x = t$, $t = 0$, and $x = c_o - M_o t$)

$$\frac{\Delta p}{q} = \frac{4\alpha}{M_o} \tag{18c}$$

From the pressure distributions it is possible to calculate the indicial lift coefficient $C_{L_\alpha}(t)$ as a function of M_o and t.

Since

$$C_{L_\alpha}(t) = \frac{1}{c_o}\int_o^{c_o} \frac{\Delta p}{q\alpha}\, dx$$

the following results are obtained:

<u>First time interval</u> $0 < t < \frac{c_o}{1+M_o}$

$$C_{L_\alpha}(t) = \frac{4}{M_o} \tag{19a}$$

<u>Second time interval</u> $\frac{c_o}{1+M_o} < t < \frac{c_o}{M_o-1}$

$$C_{L_\alpha}(t) = \frac{4}{\pi}\left[\frac{1}{M_o}\left(\frac{\pi}{2} + \arcsin\frac{c_o - M_o t}{t}\right) + \frac{1}{\sqrt{M_o^2-1}} \arccos\frac{t+M_o c_o - tM_o^2}{c_o}\right.$$

$$\left. + \frac{1}{M_o c_o}\sqrt{t^2 - (c_o - tM_o)^2}\right] \tag{19b}$$

<u>Third time interval</u> $\frac{c_o}{M_o-1} < t$

$$C_{L_\alpha}(t) = \frac{4}{\sqrt{M_o^2-1}} \tag{19c}$$

These results have been discussed in reference 7 for values of M_o greater than one. They still hold, however, for sonic flight speeds and, in fact, can be reduced to the expressions:

<u>First time interval</u> $0 < t < \frac{c_o}{2}$

$$C_{L_\alpha}(t) = 4 \qquad (20a)$$

Second time interval $\frac{c_o}{2} < t$

$$C_{L_\alpha}(t) = \frac{4}{\pi}\left(\frac{\pi}{2} + \arcsin\frac{c_o - t}{t} + 2\sqrt{\frac{2t - c_o}{c_o}}\right) \qquad (20b)$$

The indicial lift coefficient is seen to be constant and equal to 4α up to the time $t' = \frac{c_o}{2a_o}$ or up to the time required to travel one-half chord. Following this first time interval the indicial function rises monotonically, reaching an infinitely large value as time increases. The growth of $C_{L_\alpha}(t)$ is, of course, in agreement with the fact that the steady-state load coefficient becomes infinitely large in linear theory for $M_o=1$. This means that the theory cannot be used to predict the complete extent of the $C_{L_\alpha}(t)$ variation with time but that during the earlier part of the motion the assumptions remain valid.

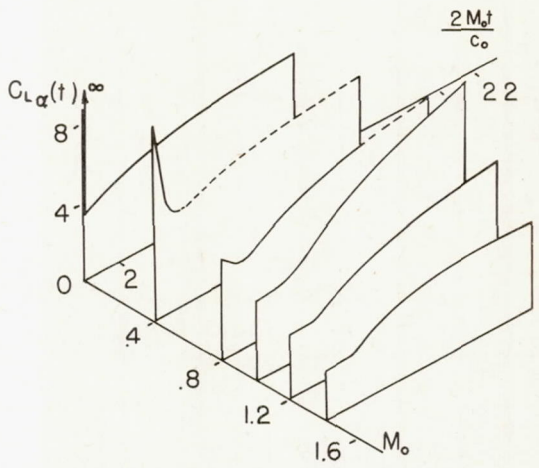

Figure 3.- Indicial-lift-curve slope for Mach numbers between 0 and 1.4 shown to time required to travel 12 half-chord lengths.

In figure 3, curves of $C_{L_\alpha}(t)$ are plotted as functions of $\frac{2M_o t}{c_o}$ for values of $M_o=1$ as given by equations (20a), (20b), and $M_o=1.2$, $M_o=1.4$ as given by equations (19a), (19b), and (19c). Also included in the figure are variations of $C_{L_\alpha}(t)$ for $M_o=0$ as calculated from Wagner's results (reference 8) by R. T. Jones (reference 9) and also for $M_o=0.8$. The derivation of results leading to the $M_o=0.8$ curve will be given subsequently in this paper. The value of $C_{L_\alpha}(t)$ at $M_o=0.4$ for a short interval of time is also drawn. The dashed portions of the curves were not calculated but were drawn to agree with the known asymptotic value of the lift function.

Application of the indicial lift function at $M_o=1$.- Once the indicial lift function is known, it is possible to determine the lift corresponding to a given variable motion. Consider, as an idealized example, the case where the airfoil experiences an abrupt rising and sinking motion at regular time intervals. Such a motion involves abrupt plus and minus angles of attack without rotation or pitching so that $\alpha(t')$ is given by the meander or square-wave function shown in figure 4(a). In this example the variation of α is such that the curve for $C_L(t')$ can be calculated easily. In figure 4(b) $C_L(t')$ is shown for the case in which the discontinuities occur at intervals of time equal to c_o/V_o, that is, after each chord length of travel. The principal point of interest in this example is the fact that such a motion yields no excessive value of lift or perturbation velocities and the entire analysis is within the framework of linear methods.

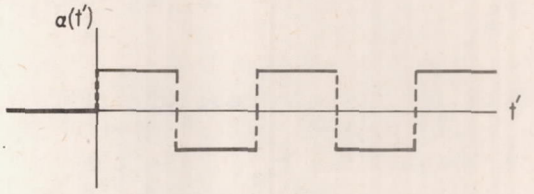

(a) Impressed angle of attack.

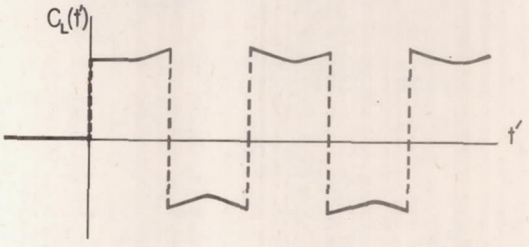

(b) Resulting variation of lift.

Figure 4.- Lift resulting from square-wave angle-of-attack variation.

When the variable motion is more complex in character the lift coefficient can be expressed by means of Duhamel's integral. Corresponding to the angle-of-attack variation $\alpha(t')$ as a function of time, the lift coefficient $C_L(t')$ is given by the expression

$$C_L(t') = \frac{d}{dt'} \int_o^{t'} C_{L_\alpha}(t'-\tau') \, \alpha(\tau') \, d\tau' \qquad (21)$$

In analysis related to equation (21) it is convenient to employ techniques associated with the use of the Laplace transformation. (See reference 10.) Thus, if the Laplace transform $\overline{f}(s)$ of the function $f(t)$ is defined by the relation

$$\bar{f}(s) = \int_0^\infty e^{-st} f(t)\, dt$$

then equation (21) can be rewritten in the form

$$\bar{C}_L(s) = s\bar{C}_{L_\alpha}(s)\bar{\alpha}(s) \tag{22}$$

Consider now the case of a lifting flat plate oscillating harmonically without pitching at a frequency ω and maximum angle of attack equal to α_{max}. Setting

$$\alpha(t) = \alpha_{max}\, e^{i\omega t} = \alpha_{max}\, e^{i\omega a_o t'} \tag{23}$$

then equation (22) yields

$$\frac{\bar{C}_L(s)}{\alpha_{max}} = \frac{4}{s-i\omega}\left(\sqrt{\frac{2}{c_o\pi}}\frac{e}{\sqrt{s}}^{-s\frac{c_o}{2}} - \operatorname{erf}\sqrt{\frac{c_o s}{2}}\right) \tag{24}$$

By straightforward manipulation, the inverse transformation of equation (24) can be shown to give

$$\frac{C_L}{\alpha_{max}} = 4e^{i\omega t}\left\{1 + \sqrt{\frac{2}{\pi\nu}}\, e^{-i\nu}\left[C(\omega t-\nu) - i\, S(\omega t-\nu)\right]\right.$$

$$\left. - 2\sqrt{\frac{2}{\pi}}\, i\, N_1(\omega t, \nu) - 2\sqrt{\frac{2}{\pi}}\, N_2(\omega t, \nu)\right\} - \frac{8}{\pi}\arctan\sqrt{\frac{2t-c_o}{c_o}} \tag{25}$$

where

$$\nu = \frac{\omega c_o}{2} = \frac{\omega' c_o}{2a_o}$$

ω' is true impressed frequency ($\alpha = \alpha_{max} e^{i\omega' t'}$).

$C(\omega t-\nu)$, $S(\omega t-\nu)$ are Fresnel's integrals (reference 11).

$N_1(\omega t, \nu)$, $N_2(\omega t, \nu)$ are integrals defined in the appendix.

If the response to a cosine variation of α is required, only the real part of equation (25) is used. Such a response in the early stages of the maneuver is shown in figure 5. For very large values of time C_L as given by equation (25) approaches the value

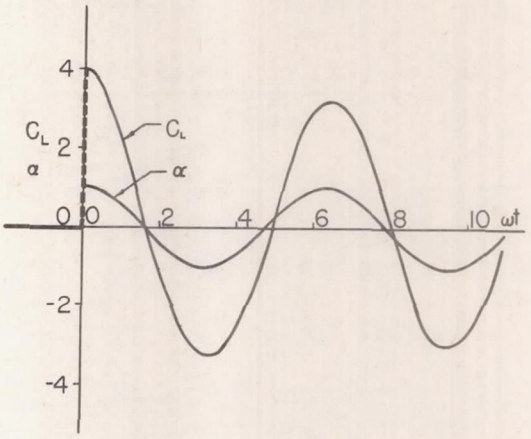

Figure 5.– Lift resulting from cosine–wave angle–of–attack variation.

$$\frac{C_L}{\alpha_{max}} = 4e^{-i\omega t}\left(\sqrt{\frac{1}{i\pi\nu}}\, e^{i\nu} - \operatorname{erf}\sqrt{i\nu}\right) \qquad (26)$$

from which both the amplitude and phase shift of C_L resulting from either an impressed sine or cosine variation of α can be readily

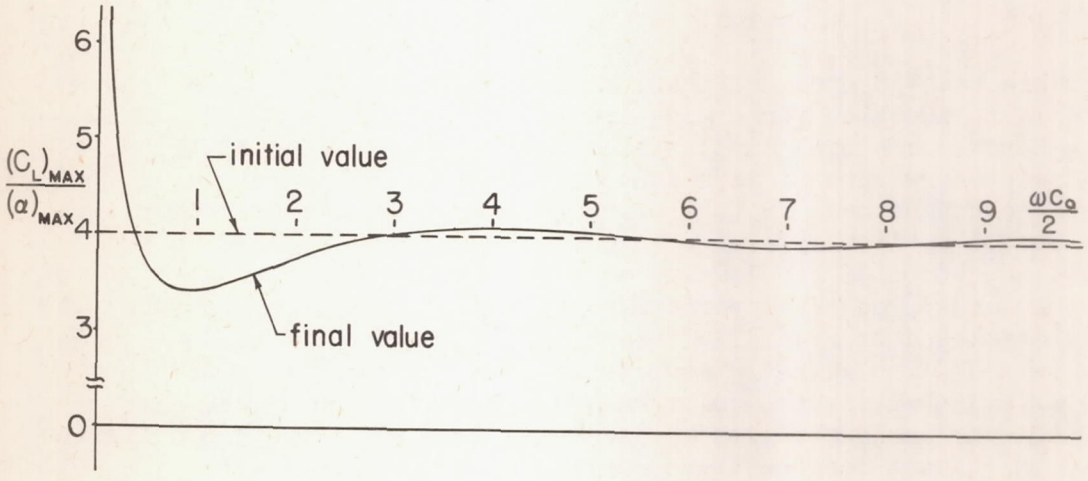

Figure 6.– Amplitude of oscillatory lift resulting from a cosine angle–of–attack oscillation (without pitching) at $M_o = 1$.

determined. Figure 6 shows the amplitude of lift oscillation corresponding to continuous angle-of-attack oscillation, as determined from equation (26), plotted as a function of $\nu = \frac{\omega c_0}{2}$. It is apparent that as ω approaches zero, C_L approaches infinity; that is, as the impressed wave approaches the "step" function (fig. 7), the lift coefficient approaches infinity. This result is in agreement with equation (20b) as t approaches infinity. As the frequency parameter ν is increased, however, the value of $C_{L_{max}}/\alpha_{max}$ is reduced and reaches a minimum of about 3.4 for a value of $\nu = 0.9$. For a speed of sound around 1000 feet per second and a wing chord of 6 feet, this would correspond to a frequency of 47.7 cycles per second, a value well within the range of practical flutter frequencies. It is interesting to note that figure 6 also shows that as the frequency of oscillation becomes large (i.e., $\nu > 3$) the value of $C_{L_{max}}/\alpha_{max}$ approaches the value 4. This is the same as the value for $C_{L_\alpha}(t)$ in the early stages following a step variation of α.

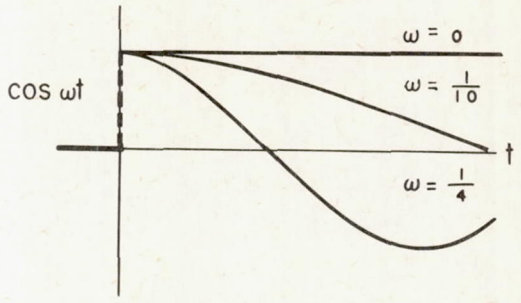

Figure 7.- Variation of cos ωt with t for various values of ω.

Unsteady State, $M_o < 1$

It has been pointed out that, in the determination of the indicial lift function for a wing traveling at subsonic speeds, the lifting-surface analogue involves the calculation of load distribution over a swept-forward wing with subsonic edges. This means that recourse cannot be made in the solution to the simple source distribution method used in reference 7 to treat the $M_o \geq 1$ case. Since, however, a portion of the leading edge in the present case is still supersonic, the problem is particularly adapted to lifting-surface methods developed by Evvard in reference 12. Figure 8 indicates, as in figure 1(b), the geometry associated with the boundary conditions. In the Evvard analysis the solutions, as in the previous case, are calculated for various regions. As an aid in identifying the different results the sketch denotes these regions by Roman numerals.

The load distributions and indicial lift functions will be given here for values of t up to the time when the characteristic from the trailing edge first crosses the leading-edge trace, that is, for

$$0 \leqq t \leqq \frac{c_o}{1-M_o}$$

or

$$0 \leqq t' \leqq \frac{c_o}{a_o(1-M_o)}$$

This period covers the time in which the wing travels $2M_o/(1-M_o)$ half chords and, since the present analysis is concerned with values of Mach number near one, will in some cases extend beyond the range of the linear theory.

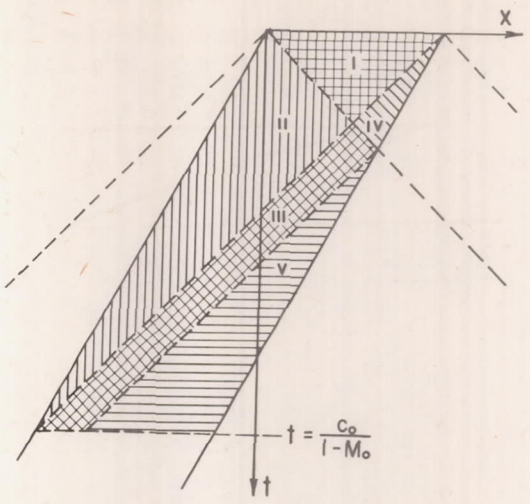

Figure 8.- Regions used in the study of subsonic unsteady lift.

The following results are obtained for load coefficient:

Region I (between lines $x=t$, $t=0$, and $x=c_o-t$)

$$\frac{\Delta p}{q} = \frac{4\alpha}{M_o} \tag{27a}$$

Region II (between lines $x=-M_o t$, $x=t$, and $x=c_o-t$)

$$\frac{\Delta p}{q} = \frac{8\alpha}{\pi M_o}\left(\frac{M_o}{1+M_o}\sqrt{\frac{t-x}{M_o t+x}} + \arctan\sqrt{\frac{M_o t+x}{t-x}}\right) \tag{27b}$$

Region III (between lines $x=c_o-t$, $x=t$, $x=-t+\frac{2c_o}{1+M_o}$, and $t=\frac{c_o}{1-M_o}$)

$$\frac{\Delta p}{q} = \frac{8\alpha}{\pi(1+M_o)}\sqrt{\frac{t-x}{x+M_o t}} + \frac{4\alpha}{\pi M_o}\left[\arcsin\frac{2x-t(1-M_o)}{(1+M_o)t} + \arcsin\frac{2(c_o-x)-t(1+M_o)}{t(1-M_o)}\right] \tag{27c}$$

Region IV (between lines $x=t$, $x=c_o-M_o t$, and $x=c_o-t$)

$$\frac{\Delta p}{q} = \frac{8\alpha}{\pi M_o}\arcsin\sqrt{\frac{x-c_o+M_o t}{t(M_o-1)}} \tag{27d}$$

Region V $\left(\text{between lines } x=-t+\frac{2c_o}{1+M_o},\ x=c_o-M_o t, \text{ and } t=\frac{c_o}{1-M_o}\right)$

$$\frac{\Delta p}{q} = \frac{16\alpha}{\pi^2(1+M_o)}\sqrt{\frac{t-x}{x+M_o t}}\left[\frac{\pi}{2} - EF(\psi,k') - KE(\psi,k') + KF(\psi,k')\right]$$

$$- \frac{2\alpha}{\pi M_o}\arcsin\frac{x}{t} + \frac{4\alpha}{\pi M_o}\arcsin\frac{2x-t(1-M_o)}{(1+M_o)t} + \frac{32\alpha K}{\pi^2(1+M_o)}\sqrt{\frac{c_o-x-M_o t}{(1-M_o^2)(x+t)}}$$

$$- \frac{2\alpha}{\pi M_o}\arcsin\frac{2c_o-t(1+M_o)}{t(1+M_o)} + N_3 \tag{27e}$$

where

$$k' = \sqrt{1-k^2}$$

$$k = \sqrt{1-\frac{2c_o}{(t+x)(1+M_o)}}$$

$$\psi = \arcsin\sqrt{\frac{x+M_o t}{c_o}}$$

$$N_s = \frac{4\alpha}{\pi^2 M_o} \int_o^{v - \frac{c_o\sqrt{2}}{M_o}} \left[\frac{1}{\sqrt{(v-v_1)(u+v_1)}}\right] \times$$

$$\left\{ \sin^{-1} \frac{(u+v_1)(1-M_o)[(v-v_1)(1+M_o)-c_o\sqrt{2}\,]+2v_1[v(1+M_o)-c_o\sqrt{2}-u(1-M_o)]}{[v(1+M_o)-c_o\sqrt{2}+v_1(1-M_o)]\,[u(1-M_o)-v_1(1+M_o)]} \right\} dv_1$$

where

$$u = \frac{1}{\sqrt{2}}(t-x)$$

$$v = \frac{1}{\sqrt{2}}(t+x)$$

$F(\psi,k)$, $E(\psi,k)$ } incomplete elliptic integrals

K, E complete elliptic integrals

In figure 9(a) the growth of pressure distribution with time is shown at subsonic speed for the period of time covered by equations (27). For purposes of comparison, pressure changes calculated from equations (18) are shown in figure 9(b) for supersonic flight velocities.

Equations (27) suffice to determine the initial growth of indicial lift coefficient at subsonic speeds. Such results were given in figure 3 at $M_o=0.8$ along with the calculated growth for about one chord length of travel at $M_o=0.4$. The value of $C_{L_\alpha}(t)$ at $t=0$ is, for all flight speeds, equal to $4/M_o$.

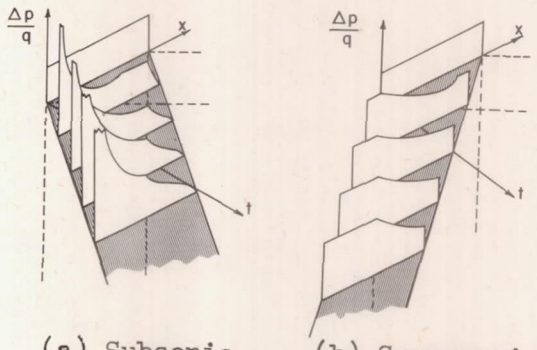

(a) Subsonic. (b) Supersonic.

Figure 9.– Pressure distribution on wings receiving sudden angle-of-attack change at $t = 0$.

Expressions for $C_{L_\alpha}(t)$ are as follows:

<u>First time interval</u> $0 < t < \frac{c_o}{1+M_o}$

$$C_{L_\alpha}(t) = \frac{4}{M_o c_o}\left[c_o - t(1-M_o)\right] \qquad (28a)$$

Second time interval $\frac{c_o}{1+M_o} < t < \frac{c_o}{1-M_o}$

$$C_{L_\alpha}(t) = \frac{4}{\pi M_o c_o}\left\{\frac{4c_o - 3t(1-M_o^2)}{1+M_o}\arctan\sqrt{\frac{2c_o - t(1-M_o^2)}{2t(1+M_o)-2c_o}}\right.$$

$$+ \pi\left(t - \frac{2c_o}{1+M_o}\right) + \frac{1+3M_o}{(1+M_o)^2}\sqrt{[2t(1+M_o)-2c_o]\,[2c_o - t(1-M_o^2)]}$$

$$+ \frac{4c_o - 2t(1+M_o)}{1+M_o}\arcsin\sqrt{\frac{t(1+M_o)-c_o}{t(1+M_o)}} - \frac{1-M_o}{1+M_o}\sqrt{c_o t(1+M_o)-c_o^2}$$

$$\left. + [2c_o - t(1+M_o)]\arctan\sqrt{\frac{c_o}{t(1+M_o)-c_o}}\right\} + \frac{1}{c_o}\int_{\frac{2c_o}{1+M_o}-t}^{c_o - M_o t}\left(\frac{\Delta p}{q\alpha}\right)_V dx \qquad (28b)$$

where $\left(\frac{\Delta p}{q\alpha}\right)_V$ is given by equation (27e).

PART III – THREE-DIMENSIONAL LINEAR PROBLEMS FOR M_o NEAR ONE

Steady State

General solutions for arbitrary Mach numbers.– Two methods of attack are available for the solution of linearized problems at sonic speeds. In the first place, solutions to equation (13) can be written formally and the extent to which these solutions satisfy the original assumption can then be investigated. In the second place, general solutions of equation (7) can be studied in the limit as M_o approaches 1. Since this latter method furnishes added information concerning the variation of the variables with M_o, it will be used first.

In linearized theory the boundary-value problems of wing theory are concerned with two separate properties of the wing: the thickness effects and the effects produced by the twist, camber, and angle of attack. The first is called the nonlifting case and the second is the lifting case. Solutions of equation (7) for $M_o \geq 1$ are given in reference (13) as follows:

In the nonlifting case

$$\varphi(x,y,z) = -\frac{1}{2\pi}\int_{\tau}\int \frac{\Delta w_o(x_1,y_1)dx_1dy_1}{\sqrt{(x-x_1)^2-\beta^2(y-y_1)^2-\beta^2z^2}} \qquad (29)$$

where $\beta = \sqrt{M_o^2-1}$ and $\Delta w_o = 2w_o$ where w_o is the vertical perturbation velocity on the wing and therefore related directly to the slope of the wing surface relative to the x axis. The integration region τ is the area on the wing within the Mach forecone from the point x, y, z.

In the lifting case

$$\varphi(x,y,z) = \frac{1}{2\pi}\left|\int_{\tau}\int \frac{\beta^2 z\ \Delta\varphi_o(x_1,y_1)dx_1dy_1}{[(x-x_1)^2-\beta^2(y-y_1)^2-\beta^2z^2]^{3/2}}\right| \qquad (30)$$

where $\Delta\varphi_o$ is the jump in the value of the velocity potential in the plane of the wing. The sign $\left|\ \right|$ denotes "finite part" of the integral and introduces special integration techniques. (See reference 13.)

Equation (29) expresses the velocity potential for the symmetrical wing in terms of an integral involving supersonic source distributions while equation (30) employs doublet distributions. In the two cases the distributions are determined from the geometry and the load distribution over the wing, respectively.

Source and doublet distribution effectiveness at infinity.- It is well known that the lift, drag, and pitching moment of a given wing may be calculated either from direct integration of the local pressures on the wing or by means of momentum considerations where the induced velocities of the wing are determined at an infinite distance and the desired forces are related to an integration over a control surface

enclosing the wing. In the three following sections the latter approach will be considered and the limiting value of drag at $M_o=1$ computed. The initial portion of this theory requires the evaluation of source and doublet effectiveness at infinity and the concept of equivalent source position, an idea which appears to have been given first by W. D. Hayes in reference 14.

Consider, as in figure 10, a point P with coordinates x, y, z lying within the induced field of a supersonic wing. The Mach forecone from P is given by the relation

$$x-x_1 = \beta\sqrt{(y-y_1)^2 + (z-z_1)^2} \tag{31}$$

where x_1, y_1, z_1 are running coordinates of a point on the surface of the cone. Introducing polar coordinates

$$y = r\cos\theta, \quad z = r\sin\theta$$

and rewriting the abscissa of P in the form

$$x = x_o+\beta r$$

it follows that the trace of the forecone in the $z_1=0$ plane is, in the limit as r approaches infinity,

$$x_1 = \beta y_1\cos\theta + x_o \tag{32}$$

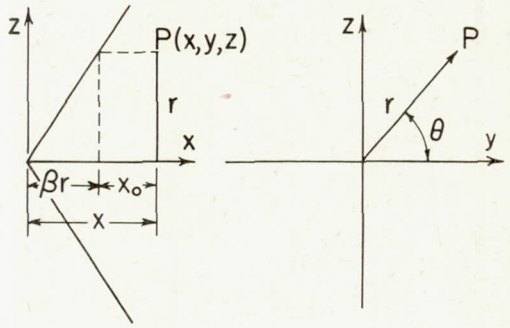

Figure 10.– Coordinates used in study of supersonic source.

It is, moreover, possible to show that the effect on the velocity potential at the point P as r approaches infinity is the same for all points $(x_1, y_1, 0)$ for which $x_1-\beta y_1\cos\theta = \text{constant}$. The value of this effect is

$$\varphi = \frac{1}{2\pi\sqrt{2\beta r(x_o-x_1+\beta y_1\cos\theta)}} \tag{33}$$

and follows from the asymptotic evaluation of the supersonic source potential

$$\varphi = \frac{1}{2\pi\sqrt{(x-x_1)^2-\beta^2(y-y_1)^2-\beta z^2}}$$

for large values of r. The potential at P for the source at $(x_1, y_1, 0)$ is thus the same as for the source shifted along the trace to $(x_1-\beta y_1 \cos\theta, 0, 0)$, the intercept of the trace on the x axis. For Mach numbers near one, equation (33) can be rewritten

$$\varphi = \frac{1}{2\pi\sqrt{2\beta r(x_0-x_1)}} \tag{34}$$

and is equivalent to the potential at P for the source at $(x_1, 0, 0)$. The induced velocities at P due to a source at $(x_1, y_1, 0)$ follow immediately, for arbitrary M_0 and for M_0 near one, from the gradients of φ in equations (33) and (34). It is important to note that equation (33) is a function of the azimuthal angle of P so that, in general, a source does not have a fixed equivalent position with respect to its potential at infinity; equation (34), however, is independent of the azimuth θ.

The source–sink potential is applicable to the study of symmetrical nonlifting wings. When lifting surfaces are to be analyzed, the doublet potential

$$\varphi = \frac{\beta^2 z}{2\pi[(x-x_1)^2-\beta^2(y-y_1)^2-\beta^2z^2]^{3/2}}$$

must be considered and the question of equivalent doublet position with respect to the potential at infinity arises. In this case the doublet position can again be shifted parallel to the trace of the Mach cone from P at infinity and the potential at P is given by the expression

$$\varphi = \frac{\beta^2 z}{2\pi[2\beta r(x_0-x_1+\beta y_1\cos\theta)]^{3/2}} \tag{35}$$

and, for Mach numbers near one,

$$\varphi = \frac{\beta^2 z}{2\pi[2\beta r(x_0-x_1)]^{3/2}} \tag{36}$$

Momentum relations.– The vectorial force $\vec{F}$ on an aerodynamic body inside a control surface S is given by the surface integral

$$\vec{F} = -\int_S \int (p-p_o)\, d\vec{S} - \int_S \int \rho \vec{V} \left[\left(\vec{V_o} + \vec{V} \right) \cdot d\vec{S} \right] \qquad (37)$$

where vector notation is used and

o subscript indicating free-stream condition

p, ρ local static pressure and density

$\vec{V}$ local perturbation velocity vector

For the purposes of the present report, equation (37) will be modified according to the assumptions of linearized theory and the surface S restricted to a semi-infinite circular cylinder of radius r, its axis of symmetry lying along the x axis, and with one face in the x=0 plane while the other face is at x=constant. (See figure 11.)

From linearized theory,

$$\frac{\rho}{\rho_o} = 1 - M_o^2 \frac{u}{V_o}$$

and

$$p - p_o = -\rho_o \left[V_o u + \frac{1}{2}(u^2+v^2+w^2) \right] + \frac{1}{2} \rho_o M_o^2 u^2$$

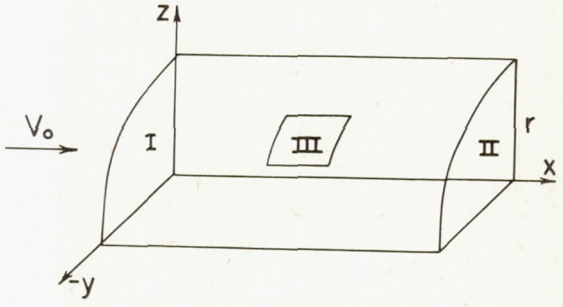

Figure 11.- Surfaces used in study of momentum.

The end faces of the cylinder may be denoted, as in the figure, by I, II, and the curved surface by III. Then in supersonic flow, if a distribution of sources is restricted to a region downstream of I, the drag D on the body corresponding to the source distribution is given by the expression

$$D = \frac{1}{2}\rho_o \int_{II} \int \left[(M_o^2-1)u^2+v^2+w^2\right] dydz-\rho_o \int_{III} \int uv_r r d\theta dx \tag{38}$$

where v_r is the radial component of the perturbation velocity. No loss in generality results, moreover, if the surface II is moved infinitely distant downstream and the radius of the cylinder is made arbitrarily large. The notation II and III will henceforth refer to this particular configuration.

If the drag of a lifting surface is to be calculated, the surface and its vorticity wake are replaced by doublet distributions and in that case the integral over region II in equation (38) is called the vortex drag of the body while region III yields the wave drag. It has also been shown (see, for example, reference 17) that the vortex drag of a supersonic wing is a function only of its span load distribution and is equal to the induced drag at subsonic speeds for the same span loading. If a finite nonlifting body is considered, each of the velocity components in region II is attenuated in such a manner that its contribution to the vortex drag is zero. The integration over region III again provides the wave drag for the nonlifting body.

The combination of the results given in this and the last section provides a method for finding the wave drag of an arbitrary body. The first step is the determination of the source-sink or doublet distribution corresponding to the body and then, by means of the principle of equivalent positions, the sources or doublets are moved to the x axis. The wave drag is then calculated from equation (38) once the induced velocities on the control surface are known. In the next section the wave drag will be written in a different form and the drag at sonic speeds will be investigated. This analysis will also provide some insight into the range of validity of the sonic theory.

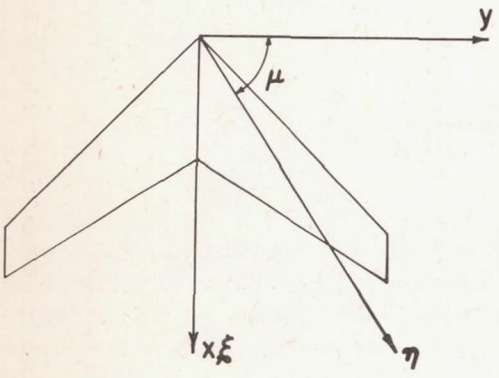

Figure 12.- System of axes in transformation equation (39).

Evaluation of wave drag as M_o approaches one.- In order to study the drag of a symmetrical body at zero angle of attack, it is convenient to consider the general expression for the velocity potential given in equation (29). Introducing first the transformation (fig. 12)

$$\left.\begin{aligned} \xi &= -y_1 \tan \mu + x_1 \\ \eta &= y_1 \sec \mu \end{aligned}\right\} \tag{39}$$

where

$$\tan \mu = \beta \cos \theta$$

equation (29) becomes

$$\varphi(x,y,z) = -\frac{1}{2\pi} \iint_{\tau} \frac{\cos \mu \, \Delta w_o(\xi,\eta) d\xi \, d\eta}{\sqrt{(x-x_1)^2-\beta^2(y-y_1)^2-\beta^2 z^2}}$$

Since, however, it has been shown that φ evaluated infinitely far away from the wing does not change if a source is moved along the line ξ=constant, it follows that the source strengths can be integrated along these lines. The second integration is then along $\eta=0$ where, from equation (39), $\xi=x_1$ and the value of the potential at an infinite distance is

$$\varphi(x,y,z) = -\frac{1}{2\pi} \int \frac{\cos \mu \, dx_1}{\sqrt{(x-x_1)^2-\beta^2 y^2-\beta^2 z^2}} \int \Delta w_o(x_1,\eta) d\eta$$

Setting

$$f(x_1,\mu) = -\cos \mu \int \Delta w_o(x_1,\eta) d\eta$$

it follows that

$$\varphi(x,r,\theta) = \frac{1}{2\pi} \int_0^{x-\beta r} \frac{f(x_1,\mu) dx_1}{\sqrt{(x-x_1)^2-\beta^2 r^2}} \tag{40}$$

and this is the same as the potential for a body of revolution with source strength per unit length given by $f(x_1)$. The induced velocities corresponding to the potential in equation (40) are found to be, after first integrating by parts and using the notation $\partial/\partial x_1 \, f(x_1,\mu) = f'(x_1,\mu)$ together with the relation $f(0,\mu) = 0$,

$$u = \frac{\partial \varphi}{\partial x} = \frac{1}{2\pi} \int_0^{x-\beta r} \frac{f'(x_1,\mu)dx_1}{\sqrt{(x-x_1)^2-\beta^2 r^2}} \tag{41}$$

and

$$v_r = \frac{\partial \varphi}{\partial r} = \frac{-1}{2\pi r} \int_0^{x-\beta r} \frac{(x-x_1)f'(x_1,\mu)dx_1}{\sqrt{(x-x_1)^2-\beta^2 r^2}} \tag{42}$$

Asymptotic values of the velocity components for large values of r are readily seen to be, after first setting $x=x_o+\beta r$,

$$u = \frac{1}{2\pi\sqrt{2\beta r}} \int_0^{x_o} \frac{f'(x_1,\mu)dx_1}{\sqrt{x_o-x_1}} \tag{43}$$

and

$$v_r = -\frac{1}{2\pi}\sqrt{\frac{\beta}{2r}} \int_0^{x_o} \frac{f'(x_1,\mu)dx_1}{\sqrt{x_o-x_1}} \tag{44}$$

Equations (43) and (44) may be used together with equation (38) to give for the value of drag the expression

$$D = \frac{\rho_o}{8\pi^2} \int_0^{2\pi} d\theta \int_0^{\infty} dx_o \int_0^{x_o} \frac{f'(x_1,\mu)dx_1}{\sqrt{x_o-x_1}} \int_0^{x_o} \frac{f'(x_2,\mu)dx_2}{\sqrt{x_o-x_2}} \tag{45}$$

Assuming that the body is of finite length so that $f'(x)=0$ for $x>l$ reversal of the order of integration yields the relation

$$D = -\frac{\rho_o}{8\pi^2} \int_0^{2\pi} d\theta \int_0^{l} \int_0^{l} f'(x_1,\mu)f'(x_2,\mu)\ln|x_1-x_2|dx_1dx_2 \tag{46}$$

If equation (46) had been derived for a body of revolution, then $f(x)$ would have been independent of the angle μ and in that case the expression for drag would reduce to the form

$$D = -\frac{\rho_0}{4\pi}\int_0^l \int_0^l f'(x_1)f'(x_2)\ln|x_1-x_2|dx_1dx_2 \qquad (46a)$$

This expression was given by von Kármán in reference 15.

For the study of the drag of a lifting surface, consider now the general expression for the velocity potential given by equation (30). The doublet distribution occupies in this case both the wing plan form and the wake since the jump in Φ exists also in the vortex wake. By use of the transformations in equation (39), equation (30) becomes

$$\varphi(x,y,z) = \frac{\beta^2 z}{2\pi}\left|\int_\tau \int \frac{\cos\mu\ \Delta\varphi(\xi,\eta)d\xi d\eta}{[(x-x_1)^2-\beta^2(y-y_1)^2-\beta^2z^2]^{3/2}}\right.$$

and, exactly as in the case of the source distribution, this can be reduced to

$$\varphi(x,y,z) = \frac{\beta^2 z}{2\pi}\left|\int \frac{\cos\mu\ dx_1}{[(x-x_1)^2-\beta^2y^2-\beta^2z^2]^{3/2}}\int \Delta\varphi(x_1,\eta)d\eta\right.$$

Setting

$$g(x_1,\mu) = \cos\mu \int \Delta\varphi(x_1,\eta)d\eta$$

it follows that

$$\varphi(x,r,\theta) = \frac{\beta^2 r\sin\theta}{2\pi}\left|\int_0^{x-\beta r} \frac{g(x_1,\mu)dx_1}{[(x-x_1)^2-\beta^2r^2]^{3/2}}\right.$$

Integrating by parts and using the fact that $g(0,\mu)=0$

$$u = \frac{\partial \varphi}{\partial x} = \frac{\sin\theta}{2\pi r}\left[\int_0^{x-\beta r} \frac{\beta^2 r^2 g'(x_1,\mu)dx_1}{[(x-x_1)^2-\beta^2r^2]^{3/2}}\right. \tag{47}$$

and

$$v_r = \frac{\partial \varphi}{\partial r} = \frac{\sin\theta}{2\pi r}\left\{\frac{1}{r}\int_0^{x-\beta r} \frac{(x-x_1)g'(x_1,\mu)dx_1}{\sqrt{(x-x_1)^2-\beta^2r^2}}\right.$$

$$\left.-\left[\int_0^{x-\beta r} \frac{(x-x_1)\beta^2 r g'(x_1,\mu)dx_1}{[(x-x_1)^2-\beta^2r^2]^{3/2}}\right]\right\} \tag{48}$$

where $g'(x_1,\mu)$ indicates $\frac{\partial}{\partial x_1} g(x_1,\mu)$. Setting $x = x_o+\beta r$ and letting r approach infinity, the asymptotic expressions for equations (47) and (48) become, if $g'(0,\mu) = 0$,

$$u = \frac{-\sin\theta}{2\pi}\sqrt{\frac{\beta}{2r}}\int_0^{x_o} \frac{g''(x_1,\mu)dx_1}{\sqrt{x_o-x_1}} \tag{49}$$

and

$$v_r = \frac{\sin\theta}{2\pi}\beta\sqrt{\frac{\beta}{2r}}\int_0^{x_o} \frac{g''(x_1,\mu)dx_1}{\sqrt{x_o-x_1}} \tag{50}$$

The relations just derived may be used in conjunction with equation (38) to give the wave drag of a lifting surface. This result takes the form

$$D = \frac{\beta^2\rho_o}{8\pi^2}\int_0^{2\pi}\sin^2\theta\int_0^{\infty}dx_o\int_0^{x_o}\frac{g''(x_1,\mu)dx_1}{\sqrt{x_o-x_1}}\int_0^{x_o}\frac{g''(x_2,\mu)dx_2}{\sqrt{x_o-x_2}} \tag{51}$$

In the wake of a lifting wing the function $g''(x_1,\mu) = 0$ and if, moreover,

$$\int_0^{c_0} g''(x_1,\mu)dx_1 = g'(c_0,\mu) - g'(0,\mu) = 0$$

reversal of integration in equation (51) yields the simpler expression

$$D = \frac{\rho_0\beta^2}{8\pi^2}\int_0^{2\pi}\sin^2\theta\, d\theta \int_0^{l}\int_0^{l} g''(x_1,\mu)g''(x_2,\mu)\ln\left|x_1-x_2\right| dx_1\, dx_2 \tag{52}$$

It is possible to draw some general conclusions from equations (46) and (52) regarding the wave drag of wings and bodies of revolution without the necessity of detailed applications to particular configurations. It is apparent immediately from equation (46a) that the wave drag of a body of revolution at zero angle of attack is independent of Mach number. This conclusion does not apply, however, to the nonlifting wing since the distribution function $f(x,\mu)$ in equation (46) contains the variable μ which, in turn, is a function of both θ and β. As M_0 approaches one, the study of the nonlifting wing is divided most conveniently into two parts, depending on the behavior of $f(x,\mu)$.

Consider first the more general situation in which $f(x,\mu)$ is not zero; that is, the case in which the number of sources does not equal the number of sinks along the line ξ = constant. This means, when M_0 is 1, that an unequal number of sources and sinks appear in the transverse or yz plane and, if equation (46) is applied, either a finite or an infinite value of drag can result. The limiting value of drag at sonic speed, obtained from integrations of surface pressures, was given by Stewart and Puckett in reference (16) for several wing plan forms, all of which had nonvanishing values of $f(x,\mu)$. If the pressure distribution is calculated, however, the local pressure coefficients are seen to become infinitely large as sonic speed is reached, even for the body of revolution, so that the assumptions of the linear theory are violated and the reliability of the drag predicted by equation (46) can in no case be assessed even though the predicted values remain finite. Equation (43) shows also that when control-surface methods are used to compute drag at $M_0 = 1$,

the x component of induced velocity increases indefinitely when $f(x,\mu)$ is not zero and that the theory is, therefore, no longer consistent.

In the very special second case, that is, when $f(x,\mu)$ vanishes for all values of θ, the analysis just presented breaks down at equation (40). It is clear, however, that in this case there are equal numbers of sources and sinks in the ξ = constant plane and the behavior of the flow field at infinity is, therefore, exactly the same as that which would have been produced by a distribution of doublets. Equations (49) and (50) give the velocities induced at infinity by an arbitrary doublet distribution. These induced velocity components are, in terms of β, one degree higher than the similar components for the nonlifting case. The values of both u and v_r can thus be expected to approach zero for all values of M_o as r approaches infinity for any flow field generated entirely by doublets or by an equal number of sources and sinks. It follows then that the linearized theory for lifting surfaces (generated entirely by doublets) and for bodies with thickness distributions such that $f(x,\mu)$ vanishes (generated by an equal number of sources and sinks in all ξ = constant planes) is entirely consistent as M_o approaches one and, in particular, for M_o equal to one. This being true, it follows immediately from equation (52) that the wave drag of a lifting system is zero at sonic speed.

Thickness solutions at $M_o = 1$.— A swept-back wing of constant chord and infinite aspect ratio is an example of a practical aerodynamic shape for which an equal number of sources and sinks occur in every yz plane. (See fig. 13.) Consider the case in which the wing cross section is diamond shaped with a slope equal to λ in a plane normal to the leading edge. Then, in a transverse plane, (section BB of fig. 13) w_o equals $\pm V_o \lambda \cos \psi$, the minus and plus signs applying, respectively, to the left and right of the ridge line. Accordingly, the solution of the problem can be written in terms of a distribution of sources, thus

$$\varphi = -\frac{1}{2\pi}\int_{\left(x - \frac{c_o}{2\cos\psi}\right)\cot\psi}^{x\cot\psi} V_o\lambda\cos\psi \ln\left[(y-y_1)^2+z^2\right] dy_1 + \frac{1}{2\pi}\int_{x\cot\psi}^{\left(x + \frac{c_o}{2\cos\psi}\right)\cot\psi} V_o\lambda\cos\psi \ln\left[(y-y_1)^2+z^2\right] dy_1 \quad (53)$$

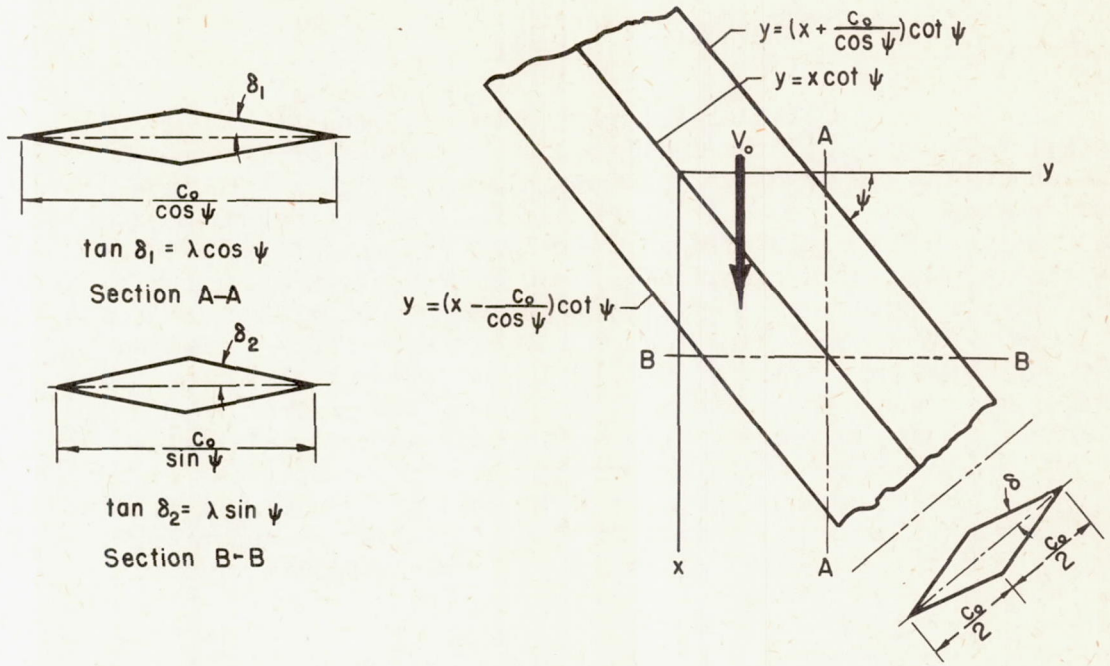

Figure 13.– Views of infinite swept wing showing coordinates.

The value of $\partial\varphi/\partial x$ can immediately be found to be

$$\frac{\partial\varphi}{\partial x} = \left(\frac{V_o\lambda\cos\psi}{2\pi\tan\psi}\right)\times$$

$$\ln\frac{\left\{\left[y-\left(x+\frac{c_o}{2\cos\psi}\right)\frac{1}{\tan\psi}\right]^2+z^2\right\}\left\{\left[y-\left(x-\frac{c_o}{2\cos\psi}\right)\frac{1}{\tan\psi}\right]^2+z^2\right\}}{\left\{\left[y-\left(\frac{x}{\tan\psi}\right)\right]^2+z^2\right\}\left\{\left[y-\left(\frac{x}{\tan\psi}\right)\right]^2+z^2\right\}} \tag{54}$$

from which it is apparent that as $r = \sqrt{y^2+z^2}$ becomes infinitely large, $\partial\varphi/\partial x$ approaches zero. In the plane of the airfoil, that is, for $z = 0$, $\partial\varphi/\partial x$ becomes

$$\left(\frac{\partial \varphi}{\partial x}\right)_o = \frac{V_o \lambda \cos \psi}{\pi \tan \psi} \ln \left[- \frac{(y \tan \psi - x - \frac{1}{2} c_o \sec \psi)(y \tan \psi - x + \frac{1}{2} c_o \sec \psi)}{(y \tan \psi - x)^2} \right]$$

and, using the definition for pressure coefficient, $C_p = - \frac{2u}{V_o}$, this becomes

$$C_p = - \frac{2\lambda \cos \psi}{\pi \tan \psi} \ln \left[\left(\frac{\frac{1}{2} c_o}{y \sin \psi - x \cos \psi} \right)^2 - 1 \right] \qquad (55)$$

Equation (55) can be derived by entirely different methods. Perhaps the most direct of these alternative derivations is the one introduced by R. T. Jones in reference 18. The general statement used in that report is that the component of translational velocity of a cylindrical body in the direction of its long axis has no effect on the motion of a frictionless fluid. Hence, the pressures over the wing shown in figure 13 are the same as those over a wing moving normal to a free stream with a velocity $V_o \cos \psi$. Using the Prandtl-Glauert correction to the thin airfoil solution of a two-dimensional, diamond-shaped, nonlifting section exposed to a free stream with velocity $V_o \cos \psi$, one obtains, for $M_o \cos \psi < 1$,

$$\varphi = - \frac{1}{2\pi} \int_{-c_o/2}^{c_o/2} \frac{w_o}{\sqrt{1 - M_o^2 \cos^2 \psi}} \ln[(x' - x_1')^2 + z^2] dx_1' \qquad (56)$$

where w_o is the vertical induced velocity on the upper side of the $z = 0$ plane and x' is measured normal to the leading edge. If this solution is referred to the axial system of figure 13 by the transformation

$$x' = x \cos \psi - y \sin \psi$$

and the integration is performed after taking the partial derivative with respect to x, the resultant expression for pressure coefficient is

$$C_p = - \frac{2\lambda \cos^2 \psi}{\pi \sqrt{1 - M_o^2 \cos^2 \psi}} \ln \left[\left(\frac{\frac{1}{2} c_o}{x \cos \psi - y \sin \psi} \right)^2 - 1 \right] \qquad (57)$$

At sonic speed this equation reduces immediately to

$$C_p = -\frac{2\lambda \cos \psi}{\pi \tan \psi} \ln \left[\left(\frac{\frac{1}{2} c_o}{x \cos \psi - y \sin \psi} \right)^2 - 1 \right] \qquad (58)$$

which is identical to equation (55). The result expressed by the two equations is, of course, not new. The significant point is that the same variation in pressure coefficient was obtained by two widely different avenues of approach and that the result obtained from the particular methods applicable to sonic speed theory is in agreement with that derived from more conventional analysis.

Lifting-surface solutions at $M_o = 1$.- It should be mentioned at this point that Robinson and Young (reference 19) have shown by means of linearized theory that supersonic triangular wings and subsonic elliptical wings of the same aspect ratio have values of lift-curve slope which approach a common and finite limit as $M_o = 1$. The present section of this report is concerned only with the study of lifting surfaces at a fixed sonic velocity but the results to be obtained are in agreement with the limiting values of reference 19.

A further application of the results in this section can be made to the case of very low aspect ratio wings at arbitrary Mach numbers. This viewpoint of the theory was first presented by R. T. Jones in reference 20 and applied to triangular wings while in reference 21 extension was made to include pointed wings on slender bodies of revolution. This duality of interpretation, that is, to all aspect ratios at sonic speed or low aspect ratios at all Mach numbers, applies to all solutions of three-dimensional problems obtained from equation (13). In the subsequent analysis, attention will be confined to swept-back plan forms of lifting surfaces with pointed vertices and thus doublets will be used exclusively.

In application, the two types of boundary conditions to be considered are as follows:

1. Boundary-value problem of the first kind, loading specified.- It is given that $\Delta u_o = u_u - u_l = 0$ over the xy plane except for the region occupied by the wing where $2u_u = -2u_l = \Delta u_o = f(x,y)$, the function being determined by the specified loading. Over all of the xy plane, the imposed conditions are $\Delta w_o = 0$.

2. Boundary-value problem of the second kind, surface specified.—

Over the xy plane, the imposed conditions are $\Delta w_o = 0$ everywhere and, except for the region occupied by the wing, $\Delta u_o = 0$. Over the region occupied by the wing $w_o = w_u = w_l = f(x,y)$ where $f(x,y)$ is determined by known camber, twist, and angle of incidence. (The delta notation again indicates the jump in the value of the variable at the $z = 0$ plane. Subscripts u and l indicate conditions on the upper and lower surface, respectively, of this plane.)

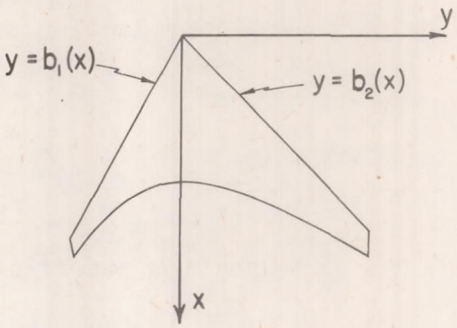

Figure 14.— Swept-back plan form with curved trailing edge.

The nature of the differential equation shows that the value of φ is a consequence of boundary conditions along lateral strips. If, as in figure 14, the two leading edges are given by the expressions $y = b_1(x)$ and $y = b_2(x)$, the velocity potential is expressible in the form

$$\varphi(x,y,z) = \frac{z}{2\pi}\int_{b_1}^{b_2} \frac{\Delta\varphi_o(x,y_1)dy_1}{(y-y_1)^2+z^2} \tag{59}$$

If the boundary-value problem is one of the first kind, the general expression for φ follows from a direct integration after noting that

$$\Delta\varphi_o(x,y) = \int_{b_1}^{y} \Delta u_o(x,y_1)dy_1 \tag{60}$$

Since, moreover, load coefficient $\Delta p/q$ is related to Δu_o by means of the equation

$$\frac{\Delta p}{q} = \frac{2\Delta u_o}{V_o}$$

it follows that the velocity potential φ can be found for any prescribed load distribution of a given plan form. The value of vertical induced velocity, evaluated at $z = 0$, then suffices to calculate the twist and angle of attack of the wing.

If the boundary-value problem is one of the second kind, the vertical induced velocity is given on the wing and the load distribution is to be found. In this case the use of equation (59) leads to the consideration of an integral equation. Since, however, this integral equation is a common one in aerodynamic theory, certain established methods may be applied to it.

After noting that $\Delta\varphi_o(x,y) = 0$ at the leading edge, integration by parts and introduction of the relation

$$\Delta v_o = \frac{\partial \Delta\varphi_o}{\partial y}$$

yields for perturbation potential the expression

$$\varphi = \frac{1}{2\pi}\int_{b_1}^{b_2} \Delta v_o(x,y_1)\arctan\frac{y-y_1}{z}\,dy_1 \tag{61}$$

In the limit as z approaches zero the derivative of φ with respect to z reduces to the form

$$w_o = -\frac{1}{2\pi}\int_{-b}^{b} \frac{\Delta v_o(x,y_1)dy_1}{y-y_1} \tag{62}$$

For a given distribution of w_o over the plan form of the wing, equation (62) represents an integral equation to be solved for $\Delta v_o(x,y)$ subject only to the condition that the Kutta-Joukowski condition is satisfied at all subsonic trailing edges. Once $\Delta v_o(x,y)$ is determined it follows that

$$\Delta\varphi_o = \int_{-b}^{y} \Delta v_o(x,y_1)dy_1 \tag{63}$$

and

$$\frac{\Delta p}{q} = \frac{2}{V_o}\frac{\partial \Delta\varphi_o}{\partial x} \tag{64}$$

In the present report the solution to the wing plan form shown in figure 15 will be presented. The value of $\Delta\varphi_o$ which satisfies

equation (62) is, in region 1

$$\Delta\Phi = -2w_o \sqrt{x^2 \tan^2 \theta - y^2} \tag{65}$$

and in region 2

$$\Delta\Phi = -2w_o \, x \tan \theta \left[E(\psi_o, k_o) - k_o'^2 F(\psi_o, k_o) \right] \tag{66}$$

where E and F are defined in the appendix and where

$$\psi_o = \arcsin \sqrt{\frac{x^2 \tan^2 \theta - y^2}{x^2 \tan^2 \theta - a_1^2}} \tag{67}$$

$$k_o' = \frac{a_1}{x \tan \theta} = \sqrt{1 - k_o^2} \tag{68}$$

The equation $y = a_1(x)$ of the trailing edge for which equation (66) is valid is given by the formula

$$a_1 = \frac{k_o'}{E_o - k_o'^2 K_o} \tag{69}$$

which expresses a_1 explicitly as a function of $\left(\frac{a_1}{x \tan \theta}\right)$. This particular choice of trailing-edge shape was used to simplify the analysis. The resulting plan form approaches a constant-chord wing as the span increases. The variation of a_1 with x is given in figure 16; and figure 17 shows the relation between aspect ratio and span.

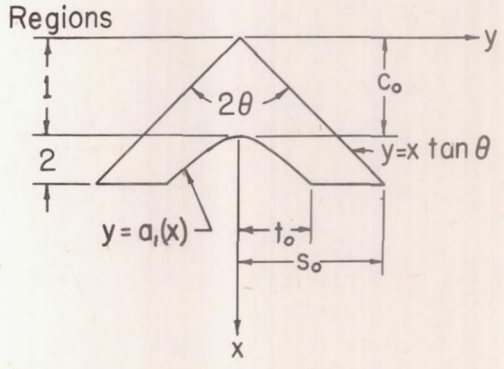

Figure 15.– Dimensions and regions used in discussion of swept-back wings.

The loading coefficient is given in the two regions (defined in fig. 15) as follows:

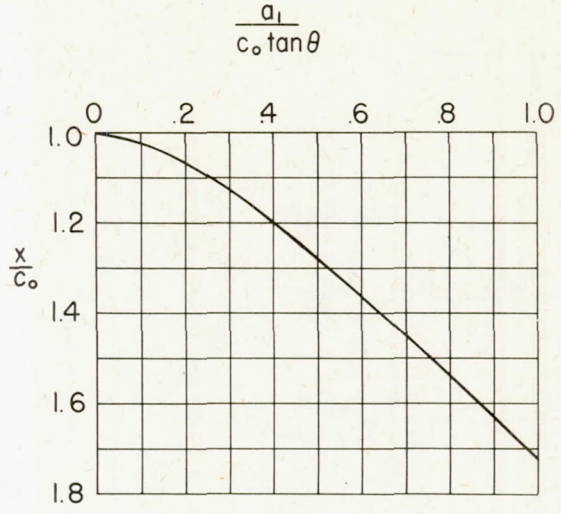

Figure 16.– Graph showing trailing-edge position of the swept-back wings studied.

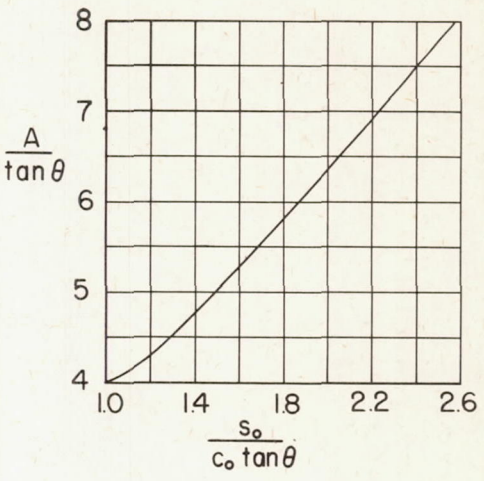

Figure 17.– Relation between aspect ratio and wing semi-span.

Region 1

$$\frac{\Delta p}{q\alpha} = \frac{4x \tan^2 \theta}{\sqrt{x^2 \tan^2 \theta - y^2}} \tag{70}$$

Region 2

$$\frac{\Delta p}{q\alpha} = 4 \tan \theta \left[E(\psi_o, k_o) + \frac{y}{x \tan \theta} \sqrt{\frac{y^2 - a_1^2}{x^2 \tan^2 \theta - y^2}} - \frac{E_o}{K_o} F(\psi_o, k_o) \right] \tag{71}$$

This load distribution is shown in figure 18 for a triangular and a swept-back wing. It is seen that the loading at sonic speed bears a close resemblance to those found at higher Mach numbers. Two similarities of note are the discontinuity in the pressure gradient at the Mach wave originating from the trailing edge of the root chord and the satisfying of the Kutta condition only where the trailing edge is subsonic. The lift and induced drag coefficients are given, respectively, by

$$\frac{C_L}{\alpha \tan \theta} = \frac{\pi}{2} \frac{A}{\tan \theta} \left(1 - \frac{t_o^2}{s_o^2}\right)$$

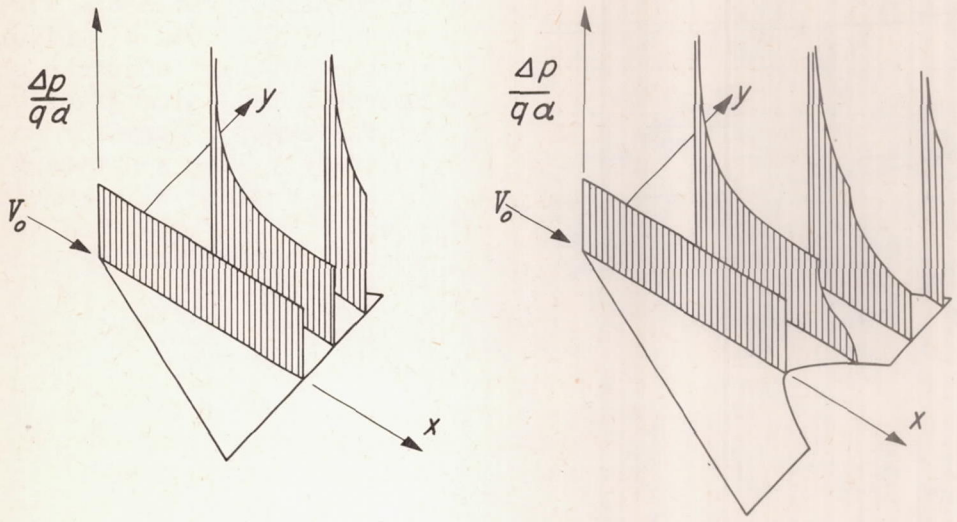

Figure 18. Pressure distributions for triangular and swept-back wings at $M_o = 1$.

and

$$\frac{C_{D_i}}{\alpha^2 \tan \theta} = \frac{A}{\tan \theta}\left[\frac{k_3^2 \pi}{4} - \frac{E_3' - k_3^2 K_3'}{(s_o/c_o \tan \theta)}\right] \tag{73}$$

where

$$k_3' = \frac{t_o}{s_o} = \sqrt{1-k_3^2}$$

These coefficients are plotted as a function of $A/\tan \theta$ in figure 19. It is shown that the values of $C_{D_i}/\alpha^2 \tan \theta$ and $C_{L_i}/\alpha \tan \theta$ for finite aspect ratio swept-back wings are always less than the corresponding values for the triangular wing $(A/\tan \theta = 4)$.

When the span of the swept-back wing becomes very large, the slope of the trailing edge approaches asymptotically the slope of the leading edge. It follows that for infinitely large aspect ratio the limiting value of the load distribution on the outboard sections should approach the value given by simple sweep theory for an infinitely long swept-back lifting surface with constant chord. This result is, in fact, a consequence of equation (71).

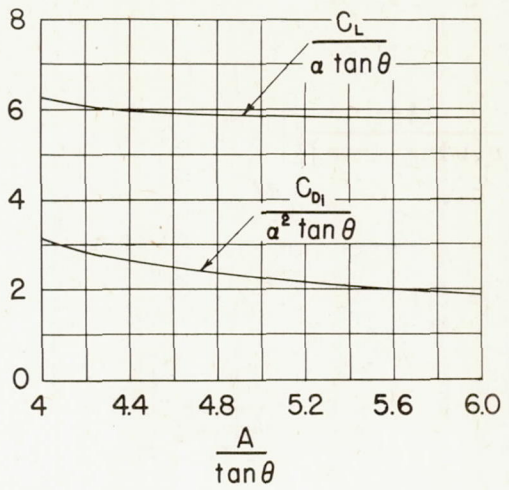

Figure 19.- Variation of lift and drag with aspect ratio for a swept-back wing at $M_o = 1$.

Ames Aeronautical Laboratory,
National Advisory Committee for Aeronautics,
Moffett Field, Calif.

APPENDIX

LIST OF IMPORTANT SYMBOLS

a_1 y coordinate of trailing edge, $y = a_1(x)$

a_o free-stream speed of sound

a local speed of sound

a^* critical speed of sound

A aspect ratio $\left[\frac{(\text{span})^2}{(\text{wing area})} \right]$

$C(u)$ Fresnel's cosine integral $\left(\int_0^u \cos \frac{\pi}{2} x^2 \, dx \right)$

c_o wing root chord

C_L lift coefficient $\left[\frac{\text{lift}}{q(\text{wing area})} \right]$

C_{L_α} $\frac{dC_L}{d\alpha}$

$C_{L_\alpha}(t)$ indicial lift coefficient

C_{D_i} induced drag coefficient $\left[\frac{D_i}{q(\text{wing area})} \right]$

D drag

D_i induced drag

$\text{erf}(x)$ error function of $x \left(\frac{2}{\sqrt{\pi}} \int_0^x e^{-\lambda^2} \, d\lambda \right)$

$E(\psi_n, k_n)$ elliptic integral of second kind $\left(\int_0^{\psi_n} \sqrt{1-k_n^2 \sin^2 \varphi} \, d\varphi \right)$

E_n $E(\frac{\pi}{2}, k_n)$

$F(\psi_n, k_n)$ elliptic integral of first kind $\left(\int_0^{\psi_n} \frac{d\varphi}{\sqrt{1-k_n^2 \sin^2 \varphi}} \right)$

K_n $F(\frac{\pi}{2}, k_n)$

K_n', E_n' elliptic integrals with moduli k'_n

k_n modulus of elliptic functions

k'_n $\sqrt{1-k^2_n}$

l length of body

M_o free-stream Mach number $\left(\frac{V_o}{a_o}\right)$

$N_1(\omega t,\nu)$ $\int_{\sqrt{\nu}}^{\sqrt{\omega t}} \left[\cos x^2\, C(\omega t-x^2) - \sin x^2 S(\omega t-x^2)\right] dx$

$N_2(\omega t,\nu)$ $\int_{\sqrt{\nu}}^{\sqrt{\omega t}} \left[\cos x^2 S(\omega t-x^2) + \sin x^2\, C(\omega t-x^2)\right] dx$

$\frac{\Delta p}{q}$ loading coefficient (pressure on lower surface minus pressure on upper surface divided by free-stream dynamic pressure)

q free-stream dynamic pressure $\left(\frac{1}{2}\rho_o V_o^2\right)$

r,θ polar coordinates in yz plane ($y = r\cos\theta$, $z = r\sin\theta$)

S Fresnel's sine integral $\left(\int_o^u \sin\frac{\pi}{2}x^2\, dx\right)$

s operational equivalent of t

s_o wing semispan

t' time

t $a_o t'$

t_o maximum distance measured parallel to y axis from x axis to trailing edge (fig. 15)

u,v,w perturbation velocity components in x,y,z directions, respectively

V local velocity

V_o free-stream velocity

v_r	radial component of perturbation velocity
x,y,z	Cartesian coordinates
α	angle of attack in radians
β	$\sqrt{\lvert 1-M_o^2 \rvert}$
γ	ratio of specific heats, for air $\gamma = 1.4$
$\Delta\varphi_o,\Delta u_o,\Delta w_o$	discontinuity in component in $z = 0$ plane
θ	semivertex angle of swept back wing
ν	$\frac{\omega c_o}{2}$
ρ_o	free-stream density
Φ	total velocity potential
φ	perturbation velocity potential
ω'	impressed frequency (reference to true time)
ω	$\frac{\omega'}{a_o}$

REFERENCES

1. von Kármán, Th.: The Similarity Law of Transonic Flow. Journal of Math. and Physics. vol. XXVI, no. 3, Oct. 1947, pp. 182–190.

2. Stewart, H. J.: The Lift of a Delta Wing at Supersonic Speeds. Quart. App. Math., vol. IV, no. 3, Oct. 1946, pp. 246–254.

3. Oswatitsch, Klaus, and Wieghardt, K.: Theoretical Analysis of Stationary Potential Flows and Boundary Layers at High Speed. NACA TM No. 1189, 1948.

4. Sauer, R.: General Characteristics of the Flow Through Nozzles at Near Critical Speeds. NACA TM No. 1147, 1947.

5. Kaplan, Carl: On Similarity Rules for Transonic Flows, NACA TN No. 1527, 1948.

6. Lamb, Horace: Hydrodynamics. Dover Publication, N.Y., 1945.

7. Heaslet, Max. A., and Lomax, Harvard: Two-Dimensional Unsteady Lift Problems in Supersonic Flight. NACA TN No. 1621, 1948.

8. Wagner, Herbert: Uber die Entstehung des dynamischen Auftriebes von Tragflügeln. Z.f.a.M.M., Bd. 5, Heft 1, Feb. 1925, S. 17-35.

9. Jones, Robert T.: The Unsteady Lift of a Wing of Finite Aspect Ratio. NACA Rep. No. 681, 1940.

10. Churchill, Ruel V.: Modern Operational Mathematics in Engineering. McGraw-Hill Book Co., N.Y., 1944.

11. Jahnke, E., and Emde, F.: Tables of Functions. Dover Publications, N.Y., 1945.

12. Evvard, John C.: Theoretical Distribution of Lift on Thin Wings at Supersonic Speeds (An Extension). NACA TN No. 1585, 1948.

13. Heaslet, Max. A., and Lomax, Harvard: The Use of Source-Sink and Doublet Distributions Extended to the Solution of Arbitrary Boundary Value Problems in Supersonic Flow. NACA TN No. 1515, 1948.

14. Hayes, Wallace D.: Linearized Supersonic Flow. North American Aviation, Inc. Rep. No. AL-222, June, 1947.

15. von Kármán, Th.: The Problem of Resistance in Compressible Fluids. (Fifth Volta Congress) Roma, Reale Accademia D'Italia, 1936.

16. Stewart, H. J., and Puckett, A. E.: Aerodynamic Performance of Delta Wings at Supersonic Speeds. Jour. Aero. Sci., vol. 14, no. 10, Oct. 1947, pp. 567-578.

17. Heaslet, Max. A., and Lomax, Harvard: The Calculation of Downwash Behind Supersonic Wings With an Application to Triangular Plan Forms. NACA TN No. 1620, 1948.

18. Jones, R.T.: Wing Plan Forms for High-Speed Flight. NACA TN No. 1033, 1946.

19. Robinson, A., and Young, A.D.: Note on the Application of the Linearized Theory for Compressible Flow to Transonic Speeds. The College of Aeronautics, Cranfield, Eng., Rep. no. 2, Jan. 1947.

20. Jones, R.T.: Properties of Low-Aspect-Ratio Pointed Wings at Speeds Below and Above the Speed of Sound. NACA TN No. 1032, 1946.

21. Spreiter, John R.: Aerodynamic Properties of Slender Wing-Body Combinations at Subsonic, Transonic, and Supersonic Speeds. NACA TN No. 1662, 1948.